Chemical Engineering Journal 115 (2005) 103–111

Chemical Engineering Journal

www.elsevier.com/locate/cej

Fluidized-bed and packed-bed characteristics of gel beads

E. van Zessen, J. Tramper, A. Rinzema, H.H. Beeftink *

Wageningen University, Food and Bioprocess Engineering Group, P.O. Box 8129, 6700 EV Wageningen, The Netherlands

Received 18 April 2005; received in revised form 25 August 2005; accepted 25 August 2005

Abstract

A liquid-fluidized bed or packed bed with gel beads is attractive as an immobilized-cell bioreactor. The performance of such bioreactors is influenced by the physical behavior of these beads. Three different but related aspects involving the drag force between particles and liquid were studied for five types of gel beads, differing in diameter and density: (1) the terminal settling velocity of a single gel bead, (2) the pressure drop over a packed bed and (3) the voidage in a liquid-fluidized bed. Qualitatively, the same trends in these aspects were observed for gel beads as for conventional solids. Quantitatively, however, these aspects were incorrectly predicted by established models (with one exception).

It was found that the drag force between gel bead and flowing liquid is smaller than that for conventional solids. As an explanation, two hypotheses are suggested. The first one attributes the drag reduction to small amounts of dissolved polymer. The second one attributes the smaller drag force to the surface nature of gel beads: gel beads contain over 95% of water and thus can be regarded as 'rigid' water droplets. Hence, the gel bead surface might show water-like properties.

As an alternative to drag-coefficient relations for conventional solids, the drag coefficient of a single gel bead in a packed or fluidized bed could successfully be described by adapting an existing relation. The success of this description facilitates a more rational design of packed and fluidized beds of gel beads.

Keywords: Gel beads; Packed bed; Liquid-fluidized bed; Drag force; Voidage; Settling velocity; Pressure drop

1. Introduction

A packed bed or liquid-fluidized bed has attractive characteristics for application as an immobilized-cell bioreactor [1,2]. Cells or enzymes can be easily immobilized in solid particles, which facilitates high biocatalyst concentrations in a bioreactor [3]. An elegant way of immobilization is to embed the catalyst in gel beads made of, e.g. κ-carrageenan, alginate or agar [4]. These beads, applied in fluidized-bed or packed-bed bioreactors, can be used for typical bio-processes like the production of ethanol [5] or lactic acid [6].

Because little is known about the hydrodynamic behavior of gel beads in liquid-fluidized beds or in packed beds, and because these highly aqueous beads might behave differently from conventional solids for these types of reactors, we studied the bead behavior in these systems. To do so, gel beads of different diameters and densities were used.

In a packed bed, upward liquid velocities can be applied up to the minimum fluidization velocity. This velocity is attained when the pressure drop equals the specific buoyant weight of the bed. In this paper, pressure-drop experiments with different kinds of gel beads are described that show that—at the same diameter and voidage—the pressure drop over a packed bed of gel beads is much lower than for conventional solids such as lead shot or glass pearls. Consequently, established pressure-drop equations, such as the Ergun equation [7] or the Foscolo equation [8] cannot be applied to predict the minimum fluidization velocity for gel beads.

In a liquid-fluidized bed, the upward liquid velocity is in between the minimum fluidization velocity and the terminal settling velocity of a single particle. At the same time, the solids hold-up ranges from ca. 0.7 (packed bed) to 0 (bead wash out); it is determined by the equilibrium between buoyancy and drag forces. In the present paper, the solids hold-up for different kinds of gel beads was determined as a function of the superficial liquid velocity. Several literature models predict this functional relation. It will be shown, however, that the empirical model of Wilhelm and Kwauk [9] with parameters values according to Richardson and Zaki [10] does not correctly

* Corresponding author. Tel.: +31 317 484204.
E-mail address: rik.beeftink@wur.nl (H.H. Beeftink).

1385-8947/$ – see front matter © 2005 Elsevier B.V. All rights reserved.
doi:10.1016/j.cej.2005.08.016

predict the fluidized-bed gel-bead hold-up from superficial liquid velocity. However, the hold-up data are predicted well if, in the model of Wilhelm and Kwauk [9], the Richardson–Zaki relation is abandoned and if parameters values are obtained by fitting instead. The more fundamental model of Grbavcic et al. [11], using independently determined parameters, was found to predict the hold-up data correctly.

Measurement of the terminal settling velocity of different kinds of gel beads showed that many models for more conventional solids underestimate the terminal settling velocity for gel beads.

The packed-bed pressure drop, the fluidized-bed solids hold-up, and the terminal settling velocity all depend on the drag force on a particle. Gel beads experience a smaller drag force than conventional particles with the same diameter and density. Two hypotheses are suggested to explain this feature. Possibly, drag reduction results from small amounts of dissolved polymer. Alternatively, drag reduction may be ascribed to differences in surface structure of the gel beads, which may be regarded as 'rigid' water droplets.

2. Materials and methods

2.1. Bead production

All κ-carrageenan gel beads (Table 1) were produced with a resonance nozzle as described by Hunik and Tramper [12]. The specific aqueous κ-carrageenan (Genugel 0909 Copenhagen Pectin Factory) solution, kept at 35 °C, was pressed through a nozzle. The drops were collected in a 80 mM KCl solution for hardening of the beads. To obtain spherical beads, butyl-acetate (Aldrich–Chemie) was layered upon the hardening solution. After hardening for approximately 2 h, beads were stored in a KCl solution to prevent the elution of counter-ions from gel beads, which otherwise would dissolve in plain tap water. Alginate beads filled with yeast were prepared with a conventional dripping method [4]. The temperature in each experiment was ambient 26 ± 2 °C.

2.2. Bead characteristics

2.2.1. Diameter

Bead diameters were determined from image analysis (CCD camera with a 50-mm Nikon macro objective). Particle images were digitized and analyzed with Genius software (Applied Imaging). For contrast, the fluid surrounding the beads (10 mM KCl) was colored with blue dextran (Pharmacia Biotech, M_w = 2,000,000 g/mol). The contrast enhancement was used for beads of type A and B, κ-carrageenan beads without any additions, as they are transparent.

2.2.2. Volume and density

To sieved gel beads, a certain amount of liquid adheres that has to be accounted for in the determination of bead volume and specific density T this end, a flask with calibrated volume V_{flask} was weighted (M_{flask}), partly filled with a blue dextran solution, and weighted again (M_1). Sieved gel beads were then added, and the flask was again weighted (M_2). The flask was the filled with a blue dextran solution up to its calibrated capacity and (V_{flask}) weighted again (M_3). After shaking for over 2 h, the 280 nm adsorption of the supernatant (A_{su}) and of the original blue dextran solution (A_{so}) were determined (Ultrospec 2000, Pharmacia Biotech). From these data, the volume and density of the gel beads were determined:

$$
\begin{aligned}
V_{\text{water added}} &= \frac{M_1 - M_{\text{flask}} + M_3 - M_2}{\rho_{\text{water}(T)}} \\
V_{\text{water total}} &= \frac{V_{\text{water added}} A_{\text{so}}}{A_{\text{su}}} \\
V_{\text{gel beads}} &= V_{\text{flask}} - V_{\text{water total}} \\
M_{\text{water adhering}} &= (V_{\text{water total}} - V_{\text{water added}})\rho_{\text{water}(T)} \\
M_{\text{gel beads}} &= M_2 - M_1 - M_{\text{water adhering}} \\
\rho_{\text{gel beads}} &= \frac{M_{\text{gel beads}}}{V_{\text{gel beads}}}
\end{aligned}
\tag{1}
$$

Diffusion of blue dextran into gel beads was not observed during a 48-h incubation in a blue dextran solution.

2.2.3. Terminal settling velocity

The split-times of gel beads settling in a glass column filled with a salt solution (6 cm inner diameter, height 1 m) were measured at different heights, starting at 50 cm from the top. Bead velocities were obtained by linear regression on height versus time data. Wall effects might become important as the particle to column diameter ratio was limited. The terminal settling velocity of type A beads was thus also determined in a wide rectangular vessel (43.5 cm × 29.5 cm × 100.5 cm, $l \times b \times h$).

2.3. Pressure drop of a packed bed of gel beads

A bed of gel beads was packed in a column (inner diameter 2.56 cm, total height 120 cm); its bottom 5 cm were filled

Table 1
Gel-bead characteristics

Bead	Mean ± σ[a] (mm)	Median (mm)	Mean ± σ[a] (mm)	Median (mm)	d_{23}[b] (mm)	Circularity	Elongation	Density (kg m^{-3})
A	1.90 ± 0.28	1.99	1.90 ± 0.28	1.99	1.97	1.03	1.18	1007.4
B	2.99 ± 0.45	3.03	2.99 ± 0.45	3.03	3.12	0.98	1.10	1005.4
C	3.14 ± 0.17	3.14	3.14 ± 0.17	3.14	3.16	1.01	1.06	1029.8
D	2.90 ± 0.42	2.83	2.90 ± 0.42	2.83	2.76	1.02	1.15	1065.1
E	4.25 ± 0.24	4.27	4.25 ± 0.24	4.27	4.27	1.00	1.13	1039.9

[a] σ, Standard deviation.
[b] Sauter mean diameter: $d_{32} = \Sigma d^3/\Sigma d^2$.

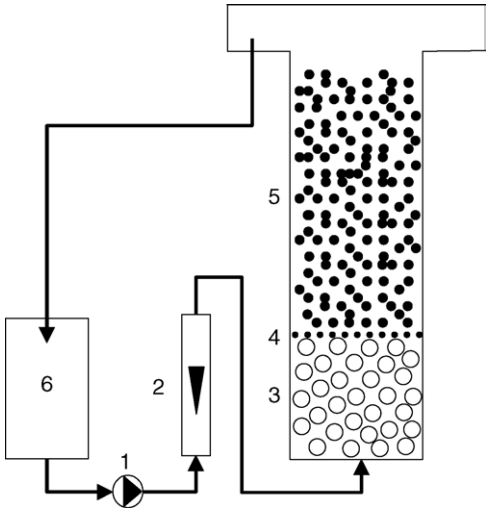

Fig. 1. Experimental lay-out for fluidization. 1, pump; 2, rotameter(s); 3, glass-pearl bed; 4, sieve plate; 5, fluidized bed of gel beads and 6, storage vessel.

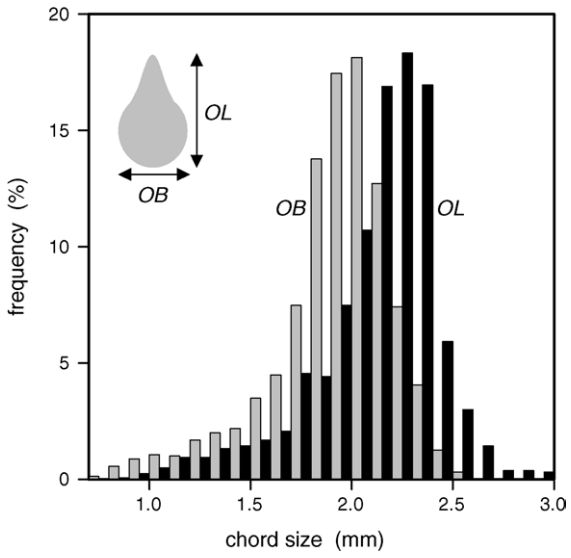

Fig. 2. Distribution of object length OL (black) and object breadth OB (grey) for type A gel beads.

with 0.8 cm glass beads for flow distribution. The pressure difference over a vertical distance was measured with a Validyne DP103 pressure transducer together with a CD23 digital transducer indicator (maximum pressure difference 140 Pa). For each set of measurements, the transducer was calibrated with a liquid manometer with water and octanoic acid (density 903 kg m^{-3}). Flow rates were measured with a calibrated rotameter (Sho-rate, Brooks). To check for wall effects, pressure-drop experiments for D type beads were also done in a 6 cm inner diameter column.

2.4. Fluidization of gel beads

Fluidization experiments were done in a glass column (inner diameter 6 cm, height 3 m; Fig. 1) into which liquid was pumped from a storage vessel. The first 10 cm of this column were filled with 0.8 cm glass pearls for flow distribution. The flow rate was measured with one or more calibrated rotameters (Sho-rate, Brooks). As the fluidized bed showed a quiescent behavior, the height of the bed could be determined visually. The solids hold-up followed from the bed height and the initial volume of the gel beads.

2.5. Predictive quality

The predictive quality of a model was expressed as the average deviation (avd) defined as:

$$\text{avd} = \frac{1}{N}\sum_{i}\left(\frac{1 - x_{i,\text{model}}}{x_{i,\text{measured}}}\right) \quad (2)$$

with x_i a model quantity and N the number of data points.

3. Results

First, the shape, diameter and terminal settling velocity of various types of gel beads are discussed. The experimental settling velocities are compared with literature predictions. Next, experimental pressure-drop data for a packed bed are compared with relevant literature predictions. The experimental results of bead fluidization, finally, are set against an empirical model [9] and a more fundamental model [11] from literature.

3.1. Gel-bead characterization

3.1.1. Shape and diameter

The size and shape of the different gel beads were evaluated with image analysis. Two important chord sizes for the shape characterization of the gel bead are the object length (OL, cf. Fig. 2), defined as the largest distance between two points on the perimeter of the object, and the object breadth (OB, cf. Fig. 2), defined as the largest distance between two points on the perimeter of the object, perpendicular to the object length. Fig. 2 shows the distributions of object length (OL) and object breadth (OB) typical for all gel beads analyzed. The OL distribution is shifted a little to higher values compared to the OB distribution, which indicates that the beads were not completely spherical. The minor deviations from sphericity were quantified (Table 1) by the object's elongation (OL/OB) and the object's circularity (i.e. the ratio between projection area and projection perimeter). An equivalent-sphere diameter was calculated from the projected bead area and was used to calculate the Sauter mean diameter d_{32} (Table 1), which was then assumed to represent the particle diameter d_p.

3.1.2. Single-particle settling velocity

The mean and median of the settling-velocity distribution for the different types of gel beads are given in Table 2. As they were almost equal, the distribution was assumed to be symmetrical for each type of gel bead.

The single-particle terminal settling velocity $v_\infty$is a key parameter in fluidization, as it is the highest superficial liquid velocity attainable in a fluidized bed. As fluidization experiments were done in a 6 cm inner diameter column, terminal-settling-velocity experiments were done in the same column for all bead

Table 2
Terminal settling velocities of gel beads (cm s^{-1})

Bead	Experimental values			Dallavalle model
	Mean ± σ[a]	Median	Wall-effect corrected	
A	1.37 ± 0.08	1.38	1.52	0.99
B	1.96 ± 0.25	2.02	2.22	1.42
C	4.41 ± 0.17	4.44	4.98	3.49
D	5.12 ± 0.24	5.12	5.69	4.89
E	5.22 ± 0.11	5.22	6.15	5.62

[a] σ, Standard deviation.

types. Since the ratio between column diameter D and gel bead diameter d_p was not large, wall effects should be accounted for. To do so, the single-particle v_∞, value for type A gel beads was also measured in a large rectangular vessel in which wall effects are negligible; it was found to be 1.518 cm s^{-1}, standard deviation ±0.065 cm s^{-1}. The ratio of the terminal settling velocity with and without wall effects was 0.90, which is close to the hindrance correction suggested by Richardson and Zaki [10]:

$$\frac{v_{\infty,\text{with wall effects}}}{v_\infty} = 10^{-d_p/D} = 10^{-2.02/60} = 0.92 \quad (3)$$

This correlation was thus used to correct the hindered settling velocity of all other beads (Table 2). The settling velocity of a single particle in a stagnant liquid can be calculated from a dimensionless force balance that accounts for gravity, buoyancy and drag:

$$Ga = \frac{3}{4} C_d Re_p^2 \quad (4)$$

In which $Ga = d_p^3(\rho_p - \rho)\rho g/\eta^2$is the Galileo number; ρ_p the particle specific mass; ρ the fluid specific mass; g the gravity acceleration; η the dynamic viscosity; C_d the single-particle drag coefficient and $Re_p = \rho v_\infty d_p/\eta$is the particle Reynolds number.

To predict v_∞, from Eq. (4), a model for the drag coefficient is needed. Models for $C_d = f(Re_p)$ are abundantly available in literature, e.g. [13–15]. Other models directly express $Ga = f(Re_p)$ [14,17–19]. All of them predict more or less the same terminal settling velocity. Table 2 shows v_∞values for the different gel beads, calculated with the equation of Dallavalle [13], using the physical properties of the gel beads (Table 1) and the physical properties of water at 24 °C [20]. Table 2 shows the predicted v_∞, values to be considerably lower than the measured ones for all gel beads, although for beads D and E these differences were less pronounced.

Fig. 3 shows the drag coefficient calculated from the experimental values for the settling velocity according to Eq. (4) and the drag coefficient predicted according to literature models. It is concluded that published models overestimate the drag coefficient for gel beads.

3.2. Packed-bed pressure drop

The measured pressure drop over a fixed bed height for the different gel beads as a function of the Reynolds number ($Re_p = \rho U d_p/\eta$) (Fig. 4) shows features commonly observed in packed-beds: the pressure drop increases with Re_p, decreases with particle diameter d_p, and the maximum pressure drop is highest for high-density gel beads.

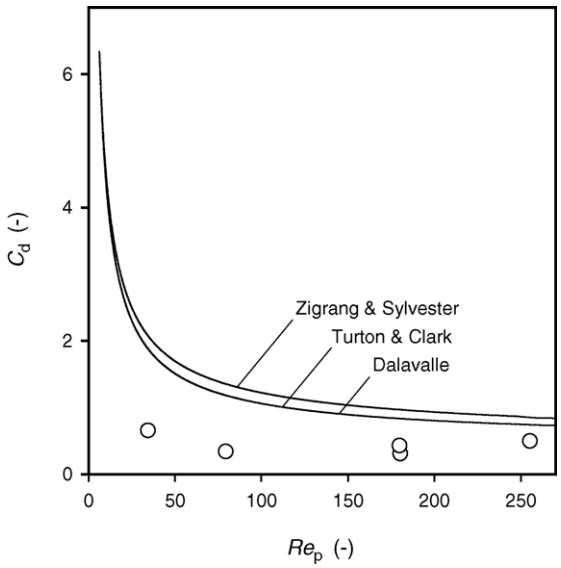

Fig. 3. Drag coefficient for gel bead particles settling in stagnant water as a function of the particle Reynolds number (physical properties: Table 1). Experimental values (◯) and model predictions according to the models by Dallavalle [13], Turton and Clark [17], and Zigrang and Silvester [16].

The model of Ergun [7] is commonly used for the prediction of pressure drop over packed beds. Foscolo et al. [8] adapted the Ergun model by introducing a voidage-dependent tortuosity. This model predicts drag forces acting on individual particles, both for a packed bed and for a stagnant liquid. Both models were found to overestimate the pressure drop over the packed bed of gel beads (Fig. 4).

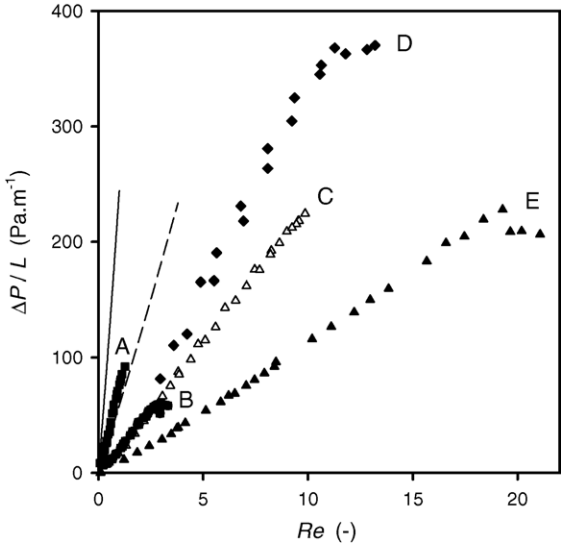

Fig. 4. Pressure drop over a packed bed of gel beads (Table 1) as a function of the Reynolds number. Column diameter 2.54 cm. (■) gel bead A; (●) gel bead B; (△) gel bead C; (♦) gel bead D; (▲) gel bead E; (—) Foscolo model, calculations for gel bead A and (- - -) Foscolo model, calculations for gel bead B.

The large discrepancy between measured and predicted pressure drops can be elucidated by considering the drag force on a single particle in the bed. A good measure for this drag force is the drag coefficient C_d. This drag coefficient can be related to the pressure drop ΔP per unit bed height L (Appendix A):

$$C_d = \frac{4}{3}\left(\frac{\Delta P}{L}\right)\left(\frac{\varepsilon^3}{1-\varepsilon}\right)\frac{d_p}{\rho U^2} \quad (5)$$

with ε is the voidage and U is the superficial liquid velocity. In the models by Ergun and by Foscolo, the drag coefficients are given by (Appendix A):

$$C_d = \frac{4}{3}\left(\frac{100}{Re(1-\varepsilon)} + 1.75\right) \quad \text{(Ergun)}$$
$$C_d = \frac{4}{3}\left(\frac{17.3}{Re} + 0.336\right)\varepsilon^{-1.8} \quad \text{(Foscolo)} \quad (6)$$

The experimental drag coefficient for gel beads A and D was calculated with Eq. (5) and compared to model predictions according to Eq. (6) as a function as a function of the hydraulic Reynolds number: $Re_h = (2/3)(1-\varepsilon)Re_p$ (Fig. 5): the drag that is experienced by a single gel bead in a packed bed is smaller than predicted by Ergun's and Foscolo's equations.

As the ratio of the particle diameter to the column diameter is less than 10 for gel beads B and C, the drag coefficient of these beads might be influenced by wall effects and they are omitted from Fig. 4. For gel beads A and B, this diameter ratio is 10 or larger. A wall effect will be present when the C_d values for data corresponding with the 6 cm diameter column are smaller than those for data corresponding with the 2.54 cm diameter column. Fig. 5 shows the opposite, and consequently a wall effect is not obvious, which remains unexplained.

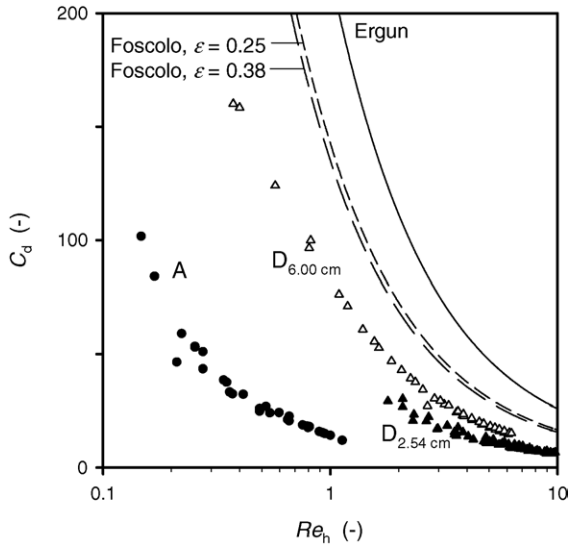

Fig. 5. Single-particle drag coefficients in a packed bed of identical particles as function of the hydraulic Reynolds number. Experimental data: (●) gel bead A; (▲) gel bead D, column diameter 2.54 cm; (△) gel bead D, column diameter 6 cm. Model predictions: (- - -) Foscolo [8], $\varepsilon = 0.25$; (– –) Foscolo [8], $\varepsilon = 0.38$; (—) Ergun [7].

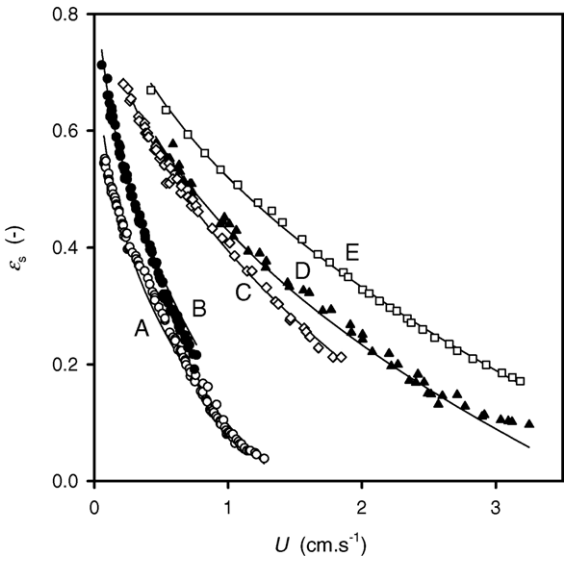

Fig. 6. Gel bead hold-up in a fluidized bed as a function of the superficial velocity. Data and description with the Wilhelm and Kwauk model ([9]; for fitted parameters see Table 3). (●) Gel bead A; (◯) gel bead B; (◊) gel bead C; (▲) gel bead D; (□) gel bead E.

3.3. Fluidization of gel beads

The gel beads from Table 1 were fluidized by the appropriate salt solutions and their hold-up was measured as a function of the superficial liquid velocity U (Fig. 6). The hold-up for each bead type was found to decrease with the superficial liquid velocity U; it increased with bead density ρ_p (type C versus type B), and with the terminal settling velocity $v_\infty$of the beads.

Experimental data for particulate bed expansion were correlated by Wilhelm and Kwauk [9] with an empirical equation:

$$U = k\varepsilon^n \quad (7)$$

with k and n empirical parameters. Table 3 gives k and n values from a satisfactory fit of Eq. (7) to the experimental data (Fig. 6).

Richardson and Zaki [10] showed that $k = v_\infty$and $n = f(Re_p)$. A comparison between k and v_∞(Table 3), however, shows that $k < v_\infty$for gel beads For $\varepsilon \to 1$, $U \to v_\infty$should be expected, but extrapolation gives a lower value. This fact has previously been reported for liquid fluidization of glass pearls, [21,22,11]. This kind of liquid-fluidized-bed expansion is one of four types defined by Di Felize [23]. The current bed expansion features two regimes. At low ε values, the relation $\varepsilon = f(U/v_\infty)$is lin-

Table 3
Fitted parameters values for liquid fluidization of gel beads according to Wilhelm and Kwauk [9], Eq. (7) and Rowe [25], Eq. (8)

Bead	Wilhelm and Kwauk		Rowe
	K	n	n
A	1.31 ± 0.03[a]	2.29 ± 0.05	3.06
B	1.40 ± 0.03	3.33 ± 0.06	2.79
C	3.16 ± 0.08	2.29 ± 0.04	2.61
D	3.77 ± 0.07	2.35 ± 0.06	2.61
E	4.67 ± 0.08	2.10 ± 0.04	2.55

[a] 95% confidence interval.

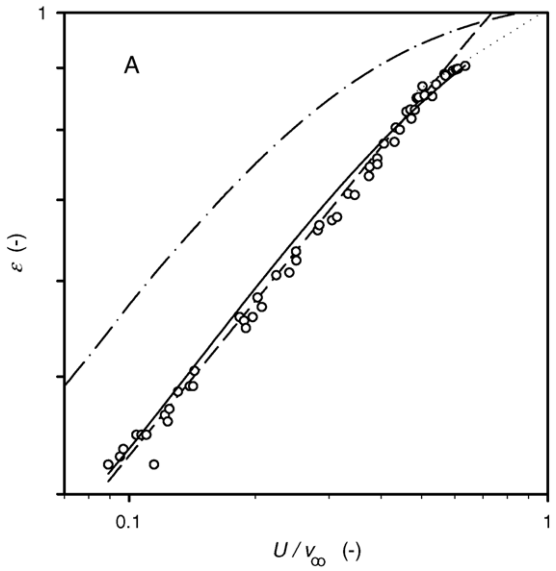

Fig. 7. Voidage for gel bead D as a function of the dimensionless velocity expressed as superficial velocity over terminal settling velocity, i.e. U/v_∞. (◯) experimental data; (—) model of Grbavcic [11] (U_{mf} = 0.358 cm s^{-1}; v_∞ = 5.12 cm s^{-1}; ε_{mf} = 0.38); (- - -) model of Wilhelm and Kwauk [9] with fitted constants; (–.–) model of Grbavcic [11] for conventional solids (U_{mf} = 0.18 cm s^{-1}, v_∞ = 4.4 cm s^{-1}, ε_{mf} = 0.38, d_p = 2.76 mm, ρ_s = 1065 kg m^{-3}).

ear on a log–log scale (Fig. 7) and extrapolation to $\varepsilon = 1$ gives $U/v_\infty < 1$. At higher ε values, the slope of $\varepsilon = f(U/v_\infty)$is smaller and extrapolation to $\varepsilon = 1$ gives $U/v_\infty < 1$(Fig. 7). In our data, this second regime is hardly present. Experiments at higher voidages were omitted, because the bed height could not be clearly determined.

Table 3 shows fit values for parameter n in Eq. (7), and predictions according to Rowe [25]:

$$n = \frac{4.7 + 0.4112 Re_p^{0.75}}{1 + 0.175 Re_p^{0.75}} \tag{8}$$

For all beads except B, the fitted n value was smaller than literature estimates; literature models thus are inappropriate to predict gel bead hold-up.

The relationship between voidage and superficial velocity as described by Eq. (7) does predict our data satisfactorily, provided the empirical constants are known. However, in the preceding paragraphs it was demonstrated that these constants cannot be determined from literature models.

An alternative to Eq. (7) is the more fundamental model of Grbavcic et al. [11], who predict voidage in liquid-fluidized beds without any adjustable constants. Their model uses the minimum fluidization velocity U_{mf}, the voidage at the onset of fluidization ε_{mf}, and the terminal settling velocity as parameters, which are easy to measure:

$$U = U_{mf} \sqrt{\frac{\varepsilon^3(1-\varepsilon)}{\varepsilon_{mf}^3(1-\varepsilon_{mf})} \frac{C_{d,mf}}{C_d}} \tag{9}$$

with:

$$\frac{C_d}{C_{d,mf}} = 1 - c_2 + \frac{1}{\lambda}\sqrt{1 - \left[\frac{\lambda(\varepsilon - \varepsilon_{mf})}{1-\varepsilon_{mf}} + c_1\right]^2}$$
$$c_1 = \left(1 + \left[\frac{U_{mf}^2}{v_\infty^2 \varepsilon_{mf}^3}\right]^2\right)^{-0.5} \tag{10}$$
$$c_2 = \frac{c_1 + \lambda}{\lambda}$$
$$\lambda = -c_1 + \sqrt{1 - c_1^2}$$

The constants, c_1, c_2 and λ are functions of the minimum fluidization velocity, the voidage at the onset of fluidization and the terminal settling velocity.

An interesting aspect of the Grbavcic model is the fact that it uses as parameters a single-particle characteristic, the terminal settling velocity, and two packed-bed characteristics: packed bed voidage at the onset of fluidization and the minimum fluidization velocity, which is equal to the maximum velocity through a packed bed. The packed bed voidage has to be determined experimentally, regardless of the kind of particles used. Although literature models fail to predict $v_\infty$and U_{mf} for gel beads, as shown above, these parameters can be easily determined.

Table 4 gives the predictive quality avd of Eqs. (9) and (10), as well as the minimum fluidization velocity and voidage, the terminal settling velocity of the different gel beads, and c_1, c_2 and λ. As a typical example, Fig. 7 shows the measured voidage, and the voidage predicted by Eqs. (9) and (10) with the constants given in Table 4, as a function of the ratio of superficial velocity to v_∞, for type D gel beads. In view of avd <0.05 for all gel beads and in view of Fig. 7, it is concluded that Grbavcic's model [11] predicts the experimental data well, although it slightly overestimates the voidage in the intermediate regime.

The empirical model by Wilhelm and Kwauk, Eq. (7), and the fundamental model by Grbavcic, Eq. (9) were both found adequate in describing gel bead hold-up as a function of superficial liquid velocity. The advantage of Eq. (7) is its mathematical simplicity. However, fluidization data are necessary to get the empirical constants. For application of Grbavcic's model, estimates of terminal settling velocity, minimum fluidization velocity and the voidage at this velocity suffice.

Table 4
Constants from Eqs. (9) and (10) for voidage calculation in liquid-fluidized beds and predicting quality (average deviation, avd)

Bead	Bead characteristics[a]			Constants in Eq. (10)			
	ε_{mf}	U_{mf}	U_t	C_1	C_2	λ	Avd
A	0.25	0.065	1.38	0.990	−0.164	−0.850	0.040
B	0.35	0.080	2.02	0.999	−0.038	−0.963	0.050
C	0.31	0.216	4.44	0.996	−0.086	−0.918	0.019
D	0.38	0.358	5.12	0.996	−0.095	−0.910	0.022
E	0.32	0.400	5.22	0.983	−0.231	−0.798	0.018

[a] ε_{mf}, voidage at minimal fluidization velocity; U_{mf}, minimal fluidization velocity (cm s^{-1}); U_t, measured terminal settling velocity (cm s^{-1}).

4. Discussion

Drag coefficients for gel beads in fluidizeds bed were found to be smaller than those of conventional solids with the same density and diameter. These low drag coefficients were manifest in three related aspects, terminal settling velocity, packed-bed pressure drop and fluidized-bed voidage. As an explanation for the difference between gel beads and conventional solids, two hypotheses are put forward. This sections ends with the derivation of a model to predict the drag coefficient of an individual gel bead either present in a packed-bed or a fluidized bed of identical gel beads.

The drag force on a particle in a fluidized bed of identical particles depends on bed voidage according to (Appendix A):

$$C_\mathrm{d} = \frac{4}{3}\frac{\rho_\mathrm{s} - \rho}{\rho}\frac{\varepsilon^3}{u^2} d_\mathrm{p} g \tag{11}$$

To compare drag coefficients, voidages should thus be known. For gel beads, experimental values were used. For conventional solids, voidages were predicted with Grbavcic's model [11], which was found superior to other literature models. Grbavcic's model requires two input parameters: the minimal fluidization velocity was calculated by Foscolo's pressure-drop equation [8], while the terminal settling velocity was calculated with Dallavalle's model [13]. Conventional-solid voidages calculated this way were found to be smaller than gel-bead voidages in all cases (Fig. 7). Consequently, the conventional-solid drag coefficients are smaller than gel-bead drag coefficients. For a single gel bead in a stagnant liquid, drag coefficients were smaller than for conventional solids (Fig. 3); the same was found to hold for drag coefficients in packed beds (Fig. 5). Thus, for all three related aspects (v_∞, ΔP, ε), gel-bead drag coefficients were smaller than those of conventional solids such as glass pearls.

Extremely low amounts of dissolved polymer are known to reduce the drag force between a solid surface and a flowing liquid [24]. In our experiments, small amounts of the matrix polymer of the gel beads, κ-carrageenan, will have been present in the liquid and may have reduced the drag force. Alternatively, the rather aqueous nature of gel beads may have been decisive. Gel beads contain water in excess of 95% and thus can be considered as 'rigid' droplets. Water flowing along the aqueous gel-bead surface may thus experience a relatively small drag force.

Most literature models were found to predict the drag coefficient for gel beads incorrectly, with Grbavcic's model for fluidized beds as an exception [11]. Since Grbavcic's model does not predict packed-bed drag coefficients, an alternative for both fluidized and packed beds is developed. Since $C_\mathrm{d} = f(\Delta P)$ in a bed of particles (Appendix A), a pressure-drop relation such as the Ergun equation is used to model the drag coefficient for gel beads [7]. Its validity does not require the particles to be in contact and it should thus in principle be applicable to both fluidized and packed beds. Unfortunately, the predictive power of the Ergun equation for fluidized beds is limited [8]. Foscolo et al. [8] revisited the Ergun equation and presented an alternative for packed and fluidized beds. Application of Foscolo's pressure-drop equation, Eqs. (6) and (7), to gel-bead drag coefficients, however, yielded incorrect predictions (Fig. 8). We, therefore, adapted Foscolo's equation and introduced two parameters c_3 and c_4:

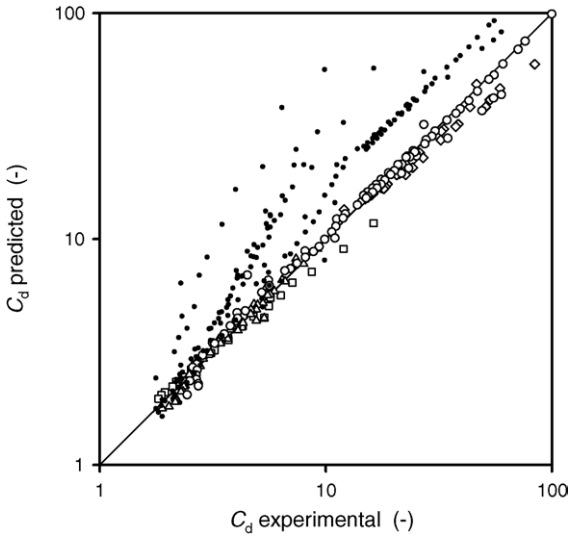

Fig. 8. Parity plot for the drag coefficient of a single gel bead in a bed of identical gel beads. Model of Foscolo et al. [8] with fitted constants. (◊) Gel bead A; (□) gel bead B; (△) gel bead C; (○) gel bead D. (●) Model of Foscolo et al. [8] with original constants.

$$C_\mathrm{d} = \frac{4}{3}\left(\frac{c_3}{Re}\varepsilon^{-c_4} + 0.336\varepsilon^{-1.8}\right) \tag{12}$$

Eq. (12) describes C_d as a function of a laminar-flow and a turbulent-flow contribution. Under turbulent-flow conditions, the dominant contribution to energy dissipation in a bed of particles are fluid vortices. Since fluid streamlines do not strictly follow the particle surface of the in the turbulent regime, it is assumed that surface structure does not influence energy dissipation. In the laminar-flow regime also, small vortices may exist; nevertheless, streamlines tend to follow the particle surface. Therefore, the turbulent part of Foscolo's model was adopted, but the laminar part was adapted to allow a fit to experimental data.

Fitting the constants c_3 and c_4 in Eq. (12) aimed at minimizing the average deviation values avd in Eq. (3), with $C_\mathrm{d} = x_i$. As experimental data, drag coefficients from pressure-drop experiments and from fluidization experiments were used, since fluidized-bed pressure drops are straightforwardly correlated with voidage (Appendix A). For the relatively small A type gel beads, small-column pressure-drop experiments could be used since wall effects were absent. For the larger beads B, C and D, fluidization experiments in a relatively large column were used. For D type beads, pressure-drop experiments above the minimal fluidization velocity were also used.

After fitting data for each bead type separately (Table 5), c_3 was found to depend on bead characteristics, while c_4 was found to be more or less constant, especially so if the sensitivity of the model for this constant is considered. Therefore, a common voidage dependency was assumed for gel beads A–D by fitting data for all beads simultaneously; resulting values are given in Table 5. Fig. 8 shows that the experimental

Table 5
Eq. (12) constants for drag-coefficient description of single beads in packed or fluidized bed

Bead	Fitted per bead type			Common voidage dependency		
	C_3	C_4	Avd	C_3	C_4	Avd
A	16.77	0.55	0.085	16.95	0.571	0.104
B	25.45	−0.0235	0.004	33.05	0.571	0.075
C	66.19	0.85	0.041	54.46	0.571	0.051
D	92.00	0.549	0.073	95.47	0.571	0.073
E	166.96	2.84	0.079	[a]	[a]	[a]

Avd, average deviation between model and data.
[a] Constants could not be satisfactorily fitted with Eq. (12).

drag coefficient is well described by Eq. (12), and the common voidage-dependency constants from Table 5. For gel bead A, c_3 is almost equal to the value in the original model of Foscolo, Eq. (7), but for the other gel beads it is increasingly larger. For the E type gel bead, the c_3 and c_4 values were quite different from other gel beads, which remains unexplained. For a packed bed and fluidized bed the effect of the voidage on the pressure drop is obtained by combining Eqs. (6) and (7) for conventional solids and by combining Eqs. (5) and (12) for gel beads A–D:

$$\begin{aligned} &\text{conventional solid}: \Delta P \sim (1-\varepsilon)\varepsilon^{-4.8} \\ &\text{gel beads A–D}: \Delta P \sim (1-\varepsilon)\varepsilon^{-2.43} \end{aligned} \tag{13}$$

The influence of the voidage on the pressure drop thus is much smaller for gel beads than for conventional solids.

5. Conclusions

For five types of gel beads, three properties were measured: terminal settling velocity of a single gel bead, pressure drop over a packed bed and voidage of a liquid fluidized bed. Although the experiments with gel beads show the same trends and characteristics as previously reported for conventional solids, pressure drop and terminal settling velocity were not correctly predicted by established models: the terminal settling velocity was higher, the pressure drop was lower. Voidage of a liquid-fluidized bed was also not well predicted by the empirical model of Wilhelm and Kwauk with parameters according to Richardson and Zaki. The more fundamental model of Grbavcic, however, was found to predict the voidage well, using a measured minimal fluidization velocity and a measured terminal settling velocity as input parameters.

It is concluded that the drag coefficient for a single gel bead, whether settling or present in a packed bed or fluidized bed, is always smaller than the drag coefficient of a conventional solid having the same diameter and density.

Two hypotheses are presented to explain the features above. The first ascribes lower drag coefficient values to the presence of dissolved polymer. The other attributes the difference between gel beads and conventional solids to a difference in surface structure: a gel bead consists for over 95% of water and can be regarded as a ‘rigid’ water droplet.

Both the drag force on a gel bead in a liquid-fluidized bed and the bed voidage are well predicted for different types of gel beads by Grbavcic’s model, which was derived for more conventional solids. Unfortunately, this model is not applicable for a packed bed. So, a different model is presented for predicting the drag coefficient of a gel bead present in a packed bed or fluidized bed of other identical gel beads. This model is based on the model of Foscolo [8] for conventional solids. The turbulent part is equal for gel beads and conventional solids. In the laminar part, however, the voidage dependency for gel beads differs from conventional solids.

Acknowledgements

We thank Arend Mulder for supplying the alginate beads. This work was financially supported by the Ministry of Economic Affairs, the Ministry of Education, Culture and Science, the Ministry of Agriculture, Nature Management and Fishery in the framework of a research program of the Netherlands Association of Biotechnology Centers (ABON).

Appendix A. Relationship between the drag coefficient of a single particle in a packed or fluidized bed of other identical particles and the pressure drop

Water flows through a bed of particles. If fluid velocities are position-independent (continuity), and if no work (W) is done by the surroundings on the fluid, a steady-state macroscopic mechanical-energy balance over a section of the bed between points 1 and 2 reads [7]:

$$\phi_\mathrm{m}\left\{\int_{P_1}^{P_2}\frac{d_\mathrm{p}}{\rho}+g(h_2-h_1)\right\}+E_\mathrm{v}\phi_\mathrm{m}=0 \tag{14}$$

with E_v the amount of mechanical energy irreversibly converted to thermal energy due to friction. If the fluid density is assumed to be pressure-independent, Eq. (14) may be solved, yielding:

$$(P_2-P_1)+\rho g(h_2-h_1)+\rho E_\mathrm{v}=0 \tag{15}$$

From the product of the force exerted by the fluid on a single particle, the fluid velocity, and the total amount of particles present, the total power dissipation $E_\mathrm{v}\phi_\mathrm{m}$ is calculated as:

$$\begin{aligned} &F_\mathrm{d}\langle v\rangle N_\mathrm{p}=C_\mathrm{d}\frac{1}{4}\pi d_\mathrm{p}^2\frac{1}{2}\rho\langle v\rangle^2\langle v\rangle N_\mathrm{p}=E_\mathrm{v}\rho u A \\ &N_\mathrm{p}=\frac{L(1-\varepsilon)A}{\frac{1}{6}\pi d_\mathrm{p}^3}\quad u=\varepsilon\langle v\rangle \\ &E_\mathrm{v}=\frac{3}{2}C_\mathrm{d}\frac{1}{2}u^2\frac{1-\varepsilon}{\varepsilon^3}\frac{L}{d_\mathrm{p}} \end{aligned} \tag{16}$$

Combining Eqs. (15) and (16) relates the drag coefficient for a single particle in a bed of identical particles to the pressure drop:

$$P_1-P_2=\rho E_\mathrm{v}+\rho g\Delta h=\frac{3}{4}C_\mathrm{d}\rho u^2\frac{1-\varepsilon}{\varepsilon^3}\frac{L}{d_\mathrm{p}}+\rho g\Delta h \tag{17}$$

In the set-up the pressure difference between point 1 and 2 is measured, and consequently the hydrostatic pressure $\rho g\Delta h$

cancels from the equation, which then simplifies to:

$$\frac{P_1 - P_2}{L} = \frac{3}{4} C_d \rho u^2 \frac{1-\varepsilon}{\varepsilon^3} \frac{1}{d_p} \tag{18}$$

Pressure drop over a packed bed due to friction between fluid and particles can be described by the Ergun equation:

$$\frac{\Delta P}{L} = \frac{150 \eta u}{d_p^2} \frac{(1-\varepsilon)^2}{\varepsilon^3} + 1.75 \frac{\rho u^2}{d_p} \frac{1-\varepsilon}{\varepsilon^3} \tag{19}$$

Pressure drop can also be described with the equation of Foscolo et al. [8]. These authors used the same basic elements, but a porosity-dependent tortuosity instead of a constant one.

$$\frac{\Delta P}{L} = \left(\frac{17.3}{Re} + 0.336 \right) \frac{\rho U^2}{d_p} (1-\varepsilon) \varepsilon^{-4.8} \tag{20}$$

At $\varepsilon = 0.4$, both models give the same pressure drop.

Eq. (18) can be combined with either Eqs. (19) or (20) to give an equation for the drag coefficient for a single particle in a packed bed of other identical particles:

$$\begin{aligned} C_d &= \frac{4}{3} \left(\frac{17.3}{Re} + 0.336 \right) \varepsilon^{-1.8} \quad \text{(Foscolo)} \\ C_d &= \frac{4}{3} \left(\frac{100}{Re(1-\varepsilon)} + 1.75 \right) \quad \text{(Ergun)} \end{aligned} \tag{21}$$

with Re_h the hydraulic Reynolds number defined as $\frac{2}{3}(1-\varepsilon)\rho U d_p / \eta$.

A.1. Liquid fluidization

The pressure drop in liquid fluidization is equal to the specific buoyant weight of the bed [8]:

$$\frac{\Delta P}{L} = (1-\varepsilon)(\rho_s - \rho) g \tag{22}$$

Combining Eqs. (22) and (18) gives the drag coefficient of single particle in a fluidized bed of identical particles:

$$C_d = \frac{4}{3} \frac{\rho_s - \rho}{\rho} \frac{\varepsilon^3}{u^2} d_p g \tag{23}$$

References

[1] F. Gòdia, S. Solà, Fluidized-bed bioreactors, Biotechnol. Prog. 11 (1995) 479–497.

[2] R.G. Willaert, G. van Baron, L. de Backer, Immobilised cell systems, in: Immobilised Living Cell Systems: Modeling and Experimental Methods, John Wiley & Sons, New York, 1996, pp. 67–97.

[3] R.H. Wijffels, R.M. Buitelaar, C. Bucke, J. Tramper, Immobilized Cells: Basics and Applications, Elsevier, Amsterdam, 1996.

[4] A.C. Hulst, J. Tramper, K. van't Riet, J.M.M. Westerbeek, A new technique for the production of immobilized biocatalyst in large quantities, Biotechnol. Bioeng. 27 (1985) 870–876.

[5] F. Gòdia, C. Casas, C. Solà, A survey of continuous ethanol fermentation systems using immobilized cells, Proc. Biochem. 4 (1987) 43–48.

[6] H. Wang, M. Seki, S. Furusaki, Characteristics of immobilized *Lactobacillus delbrueckii* in a liquid-solid fluidized bed bioreactor for lactic acid production, J. Chem. Eng. Jpn. 28 (1994) 198–203.

[7] R.B. Bird, W.E. Stewart, E.N. Ligthfoot, Transport Phenomena, John Wiley & Sons, Singapore, 1960, p. 200.

[8] P.U. Foscolo, L.G. Gibilaro, S.P. Waldram, An unified model for particulate expansion of fluidised beds and flow in fixed porous media, Chem. Eng. Sci. 38 (1983) 1251–1260.

[9] R.H. Wilhelm, M. Kwauk, Fluidization of solid particles, Chem. Eng. Prog. 44 (1948) 201–217.

[10] J.F. Richardson, W.N. Zaki, Sedimentation and fluidization. Part 1, Trans. Inst. Chem. Eng. 32 (1954) 35–53.

[11] Z.B. Grbavcic, R.V. Garic, D.z.E. Hadzismajlovic, S. Jovanvic, Variational model for prediction of the fluid-particle interphase drag coefficient and particulate expansion of fluidized and sedimenting beds, Powder Technol. 68 (1991) 199–211.

[12] J.H. Hunik, J. Tramper, Large Scale production of κ-carrageenan droplets for gel bead production: theoretical and practical limitations of size and production rate, Biotechnol. Prog. 9 (1993) 186–192.

[13] J.M. Dallavalle, Micrometrics: The Technology of Fine Particles, second ed., Pitman, London, 1948.

[14] N. Hidaka, K. Kakoi, T. Matsumoto, Correlation of solid hold-up in liquid-solid fluidized bed, J. Chem. Eng. Jpn. 27 (1994) 563–570.

[15] R. Turton, O. Levenspiel, A short note on the drag coefficient for spheres, Powder Technol. 47 (1986) 83–86.

[16] D.J. Zigrang, N.D. Silvester, An explicit equation for particle settling velocities in solid-liquid systems, AIChE J. 27 (1981) 1043–1044.

[17] R. Turton, N.N. Clark, An explicit relationship to predict particle settling velocity, Powder Technol. 53 (1987) 127–129.

[18] R.A. Kahn, J.F. Richardson, The resistance to motion of a solid sphere in a fluid, Chem. Eng. Commun. 62 (1987) 135–150.

[19] M. Hartman, V. Havlin, O. Trnka, M. Carsky, Predicting the free-fall velocities of spheres, Chem. Eng. Sci. 44 (1989) 1743–1745.

[20] R.C. Weast, Handbook of Chemistry and Physics, 59th ed., CRC Press, Boca Raton, 1979.

[21] J. Garside, M.R. Al-Dibouni, Velocity-voidage relationships for fluidization and sedimentation in solid-liquid systems, Ind. Eng. Chem. Proc. Des. Dev. 16 (1977) 206–214.

[22] J.P. Riba, J.P. Couderc, Expansion de couches fluidiseés par des liquids, Can. J. Chem. Eng. 55 (1977) 118–121.

[23] R. di Felize, Hydrodynamics of liquid fluidization, Chem. Eng. Sci. 50 (1995) 1213–1245.

[24] O. Paireau, D. Bonn, Drag reduction in liquid–liquid friction, Phys. Rev. Lett. 83 (1999) 5591–5594.

[25] P.N. Rowe, A convenient model empirical equation for estimation of the Richardson-Zaki exponent, Chem. Eng. Sci. 43 (1987) 2795–2796.